



HAL
open science

Micro-spikes formed on mesoporous silicon by UV picosecond laser irradiation

Nadjib Semmar, Abderazek Talbi, Maxime Mikikian, Arnaud Stolz, Amer
Melhem, Domingos de Sousa Meneses

► **To cite this version:**

Nadjib Semmar, Abderazek Talbi, Maxime Mikikian, Arnaud Stolz, Amer Melhem, et al.. Micro-spikes formed on mesoporous silicon by UV picosecond laser irradiation. *Applied Surface Science*, 2020, 509, pp.144820. 10.1016/j.apsusc.2019.144820 . hal-02397793

HAL Id: hal-02397793

<https://hal.science/hal-02397793>

Submitted on 11 Dec 2020

HAL is a multi-disciplinary open access archive for the deposit and dissemination of scientific research documents, whether they are published or not. The documents may come from teaching and research institutions in France or abroad, or from public or private research centers.

L'archive ouverte pluridisciplinaire **HAL**, est destinée au dépôt et à la diffusion de documents scientifiques de niveau recherche, publiés ou non, émanant des établissements d'enseignement et de recherche français ou étrangers, des laboratoires publics ou privés.

Micro-spikes formed on mesoporous silicon by UV picosecond laser irradiation

N. Semmar¹, A. Talbi¹, M. Mikikian¹, A. Stolz¹, A. Melhem¹, D. de Sousa Meneses²

¹ GREMI-UMR 7344, CNRS-Université d'Orléans, 14 rue d'Issoudun, BP 6744, 45067 Orléans Cedex 2, France

² CEMHTI-UPR 3079, CNRS-Orléans, Avenue de la Recherche Scientifique, 45100 Orléans, France

Abstract: Conical spikes with sizes ranging between 0.2 and 5 μm were formed on a mesoporous silicon surface under ultraviolet picosecond laser irradiation in ambient air. Scanning electron microscopy was employed to visualize the successive steps in the formation of the spikes. On increasing the number of shots (up to 1000) at a fluence of 400 mJ/cm^2 , an increase in the size and an enhancement in the distribution of spikes were observed. The experimental observations revealed that the formation and the growth of these structures were mainly due to material ablation and removal mechanisms. FTIR analysis on several large (5X 5 mm^2) irradiated zones showed an enhancement in the absorption coefficient mainly in the IR range from 1 to 8 μm versus the size of the microstructures.

Keywords: Mesoporous silicon; picosecond laser beam; micro-texturing; micro-spikes; FTIR spectroscopy; Reflectivity

1. Introduction

Micro and nanostructured surfaces have received great attention due to their potential in a wide range of applications such as sensor technology, surface tribology and adherence and energy harvesting. Several methods have been investigated to modify the material surfaces such as plasma treatment, ion-beam sputtering, reactive ion etching, and laser treatment [1-3]. Among these methods, laser surface treatment has attracted growing interest in recent years due to its good spatial resolution and high reproducibility on different materials such as metals, semiconductors, dielectrics and polymers [4-6]. Many types of laser sources have been employed from continuous waves (cw) to ultra-short beams, and with working wavelengths from UV to IR [7-8]. As a result of laser-matter interaction, a large variety of structures and patterns from the nano to the micro-scale have been generated depending on the laser parameters and material properties, such as laser induced periodic surface structures (LIPSS), 2D circular droplets and particular microstructures called spikes [9-14].

Silicon (Si) has been extensively used in the microelectronics industry for more than half a century. This semiconductor presents an indirect band gap of 1.1 eV that makes it transparent to wavelengths larger than 1.1 μm [15]. In other words, silicon cannot absorb light for optical wavelengths larger than 1.1 μm , which reduces its efficiency in many applications especially for solar cells and photo-detectors [16-17]. In order to enhance the optical properties of silicon (to extend the operating wavelength range), many efforts have focused on the synthesis of micro-structured silicon, or so-called black silicon [18-19]. Black silicon (BS) has been fabricated by reactive ion etching since the 1980s. During the last two decades, black silicon has also been produced using femtosecond or nanosecond laser irradiation of silicon wafers under various atmospheres (SF_6 , N_2 , H_2 , air and water) [10, 20-21]. This novel material, defined as a forest of microscopic spikes, exhibits a low reflectance and a high absorption for a wavelength spectrum extending up to 2 μm . The enhancement of the absorbance allows the design and the development of high sensitivity infrared photodetectors and photodiodes [20].

Additionally, BS opens promising applications on super-hydrophobic surfaces and microfluidic devices [22] due to its morphology that can be significantly enhanced with mesoporous structures.

Despite a smaller absorption efficiency than Si, mesoporous silicon (MeP-Si) exhibits a sponge-like nano-structure that is very useful in many potential applications, for example in gas sensing, in microelectronics and also for micro-electro-mechanical systems (MEMS) [23]. In the present work, the formation of micro-textured surfaces of MeP-Si using an ultraviolet picosecond laser fluence of 400 mJ/cm^2 was investigated in order to obtain similar surface morphologies as those reported with silicon that could lead to an enhancement in the optical properties. Particularly, the reflectivity change versus laser parameters is discussed in the second part of this work using a large-scale laser surface texturing process. As reported in a previous study [24], 400 mJ/cm^2 is a high enough fluence close to the ablation threshold that helps in the step-by-step engraving process.

2. Experimental details

Mesoporous silicon MeP-Si substrates were provided by the SiLiMiXT ® Company and fabricated from $500 \text{ }\mu\text{m}$ thick p-type $\langle 100 \rangle$ -oriented silicon wafers by electrochemical etching of around $50 \text{ }\mu\text{m}$ thickness as shown in fig1. Electrical resistivity was in the range of $10\text{-}20 \text{ m}\Omega\cdot\text{cm}$, with a porosity of about 40% and a pore size in the range of $1\text{-}10 \text{ nm}$.

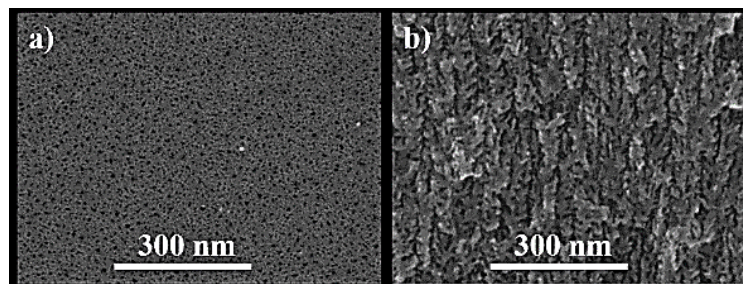


Figure 1. Top and cross section SEM views of MeP-Si substrate

A Nd:YAG picosecond linearly polarized laser generating 40 ps pulses at 10 Hz, and with a fundamental wavelength of 1064 nm was used in this work. Thanks to a fourth harmonic generator, a wavelength of 266 nm was achieved and was used to irradiate the MeP-Si substrates. A plano-convex lens with a focal length of 75 mm was used to focus the laser beam 20 mm behind the sample surface leading to a laser spot size of about $600 \text{ }\mu\text{m}$ on the sample surface. Experiments were carried out in ambient air. Scanning electron microscopy was employed to characterize the top view and tilted cross section of treated zones. ImageJ ® software was used to analyze the SEM images in order to determine the size distribution of the microstructures formed.

3. Micro-spikes formation

Figure 2 displays a sequence of SEM top views (for two magnifications) of the obtained surface morphologies of MeP-Si and the structure radius distributions as a function of the number of shots N . After only 10 shots, various irregular structures appeared randomly on the surface. An asymmetric radius distribution was observed in the range 0.4 to $1.5 \text{ }\mu\text{m}$ with a maximum probability at $0.4 \text{ }\mu\text{m}$. When N increased up to 100, the formation of larger spikes up to $2 \text{ }\mu\text{m}$ was achieved. The histogram is broadened and shows a slight increase in the most frequent size at about $0.6 \text{ }\mu\text{m}$.

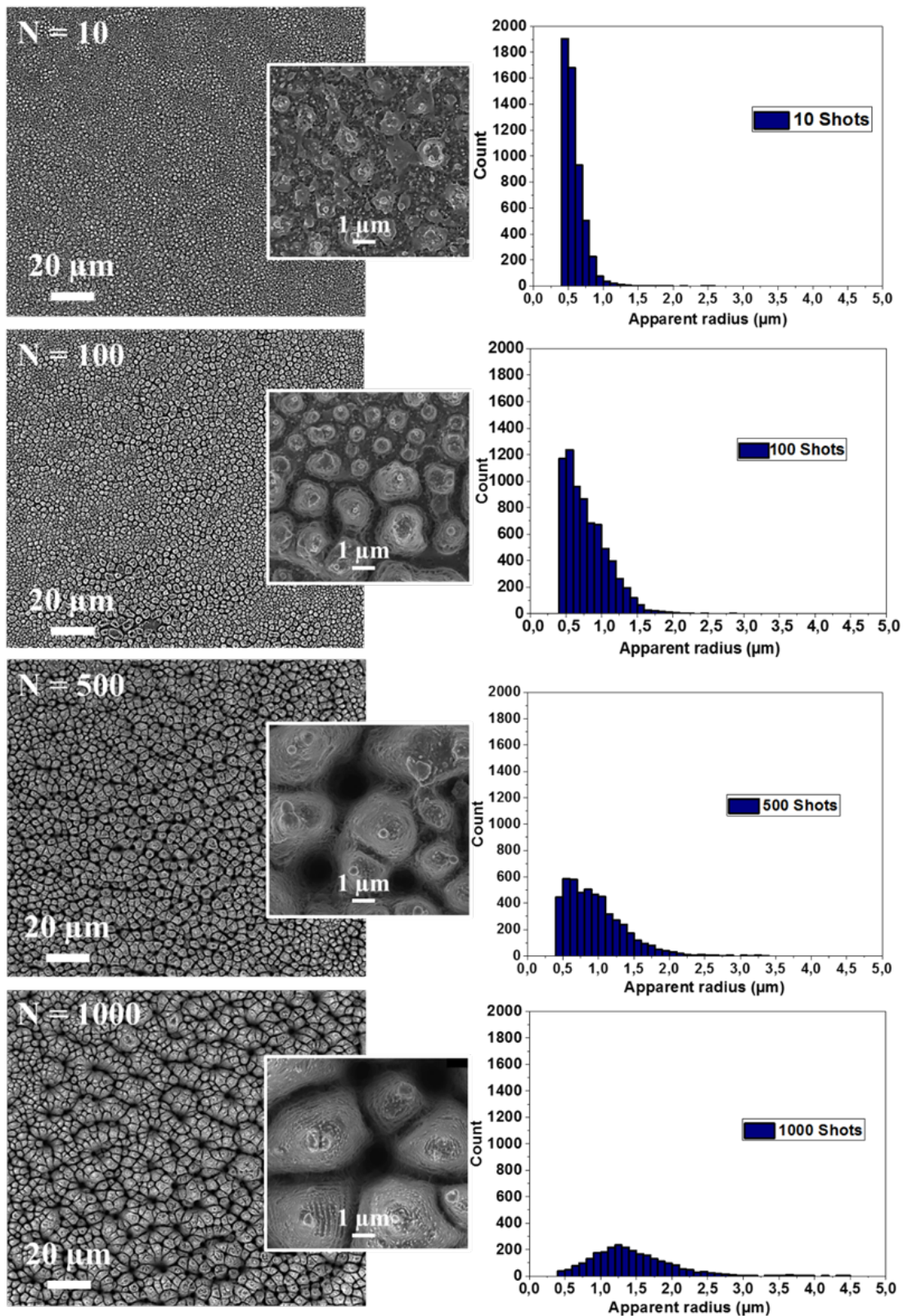


Figure 2. SEM top views and histograms of radius distribution of spikes formed on MeP-Si surface by 400 mJ/cm² ps irradiation for 10 to 1000 shots

After 500 shots, regular spikes homogeneously cover the MeP-Si surface with a radius distribution slightly shifted towards larger sizes. On increasing N to 1000, a similar global organization of bigger and deeper spikes is observed but the radius distribution exhibits a quasi-Gaussian shape showing that the most frequent apparent radius is at about 1.2 µm.

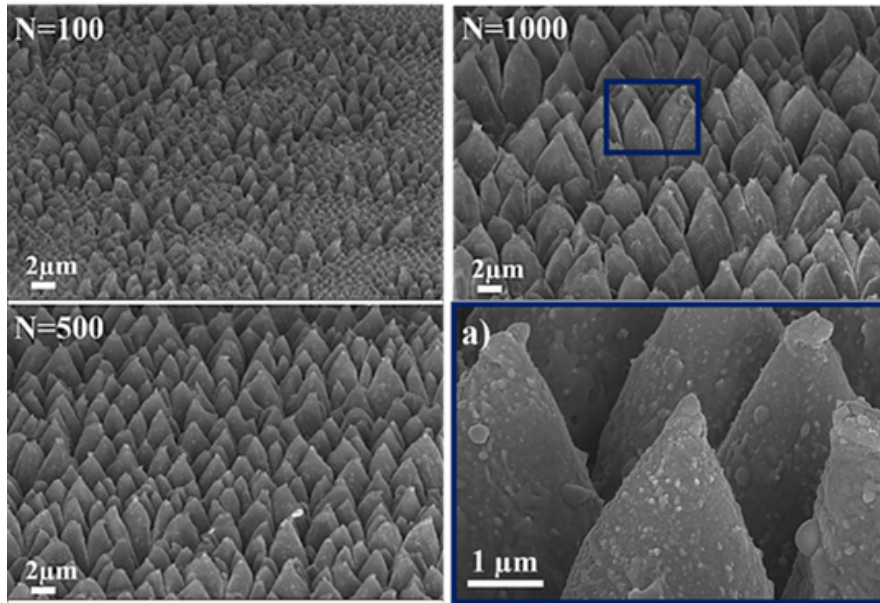


Figure 3. Tilted SEM cross section views of spikes formed for various N from 100 to 1000, a) zoom of spikes formed for N = 1000

SEM top views are a useful tool to investigate the homogeneity and the size distribution of the spikes formed. In order to examine the shape of these spikes more precisely, tilted SEM characterizations were performed for N=100, 500 and 1000 as shown in Fig 3. As already shown from the top views (Fig. 2) and the histograms, the tilted views on Fig.3 confirm that increasing N leads to an increase in the spike size and to a better homogeneity of their distribution on the surface. Between 500 to 1000 shots, quasi-uniform conical spikes are fully developed over the entire surface (Fig.3a). The depth of structures increases steadily versus N. The estimation of the ablation rate at 400 mJ/cm² returns a mean value of 12 nm/pulse over the range N = 10 to 10000. In other words for N = 100 the estimated mean depth is close to 1.0 μm and over 10.0 μm for N = 1000, as also expected from Fig. 3.

Figure 4 shows the transverse section of a spike core that exhibits almost the same morphology as untreated mesoporous silicon (Fig. 1b). However, a very thin melted phase can be observed in the valleys between spikes and on the external envelope of the spike. This melted material is made of irregular nanostructures that cover the spikes after cooling. This result indicates that, even if ablation process plays the main role in the spike formation, a thermal effect such as melting that occurs in the cooling phase also contribute to the final spike structures.

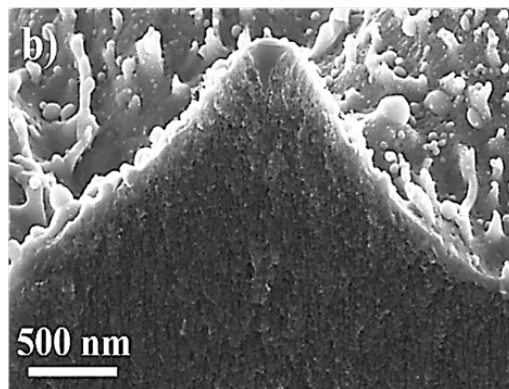


Figure 4. Typical spike core obtained at 400 mJ/cm² and 1000 shots

Despite several studies on spike formation on silicon (mainly crystalline) by fs laser irradiation, the formation mechanisms of these structures are not fully understood [17, 22, 25-26]. Sarnet et al. [18] proposed the following scenario to describe the mechanism of spike formation. First, at a low laser dose, small structures (LIPSS) [27] are formed, similar to capillary waves with a periodicity close to the beam wavelength. When the laser dose is increased, capillary waves tend to form larger and more hydrodynamically stable structures. The absorption of laser energy by these structures is not uniform: the ablation process is enhanced in the valleys between these structures, leading to an amplification of the phenomenon and to a quasi-uniform spike distribution on the surface.

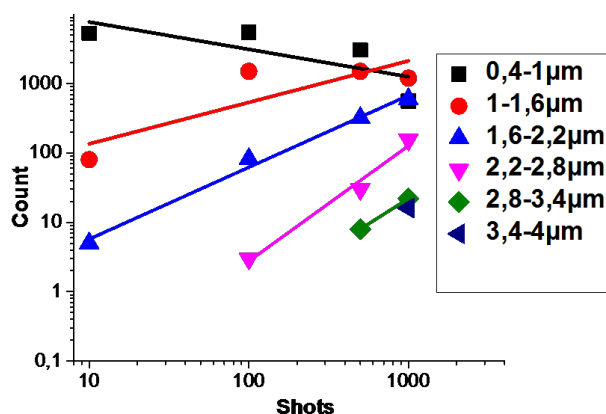


Figure 5. Spike size distribution versus N

As reported in our previous work [28], in the case of MeP-Si, the use of a relatively low fluence (with either a picosecond or a femtosecond beam) leads to LIPSS formation through the organization of nanoparticles generated after a few shots. Also, in the same work, a periodic melt material was formed but only after a high number of shots ($N > 10^4$). In contrast, when employing a relatively high fluence of 400 mJ/cm^2 above the ablation threshold of silicon (for example 60 mJ/cm^2 at 248 nm for a pulse duration of 100 fs [29]), LIPSS do not form. However, a strong ablation process is clearly achieved even after only 10 shots, changing the initial flat and smooth surface of MeP-Si into a roughened surface covered by irregular structures with sizes ranging from 0.4 to $1.0 \text{ }\mu\text{m}$ (Fig 5.). On increasing N from 10 to 100, the non-uniform ablation process occurs steadily and is maximized in the valleys between the structures formed, leading to preferential material removal in these areas. As a consequence, the ablation process digs around the flat areas leading to the birth and growth of spikes. As a result of these processes, the amount of small structures (size ranging between 0.4 - $1.0 \text{ }\mu\text{m}$) decreases with increasing N whereas the amount of larger structures (1.0 - $2.2 \text{ }\mu\text{m}$) increases. Additional shots tend to enhance the shape and uniformity of the spikes until the surface is uniformly covered with spikes with radii up to $4 \text{ }\mu\text{m}$ (Fig. 5) (500-1000 shots). Despite the similar ablation process, in comparison to the fluences employed to create BS spikes (in the range of 4 to 20 J/cm^2) [17, 29-31], spikes on MeP-Si are formed at relatively low fluence $\sim 0.4 \text{ J/cm}^2$ with a picosecond laser beam. In this case the most regular conical shape seems to be uniform for N close to 1000.

4. Optical properties evaluation of large scale processing

MeP-Si materials could be a good candidate for energy harvesting namely in photovoltaic devices [31-33]. To assess the changes in the material optical properties induced by the ps laser irradiation, large scale processing was used to texture a $5 \times 5 \text{ mm}^2$ MeP-Si surface.

To link this case of surface treatment to the previous section it is important to determine the equivalent working fluence and number of laser shots (N). The simple formula that correlates the overlap (ov) to the X scan speed (V_x), the beam diameter (D) and the laser frequency (f), also returns the number of shots as described in the following equation:

$$ov (\%) = 100 \cdot \left(1 - \frac{V_x}{f \cdot D}\right), \quad \text{and} \quad N = D \cdot \left(\frac{f}{V_x}\right) \quad (1)$$

The process parameters (energy, translation speed and translation step) are summarized in Figure 6 that shows SEM images, revealing the changes induced by increasing the beam energy from 1 mJ/pulse to 5 mJ/pulse (i.e. for $D = 800 \mu\text{m}$, F is increased from 200 to 1000 mJ/cm^2). The laser sweeps the surface at a fixed scan speed of 200 $\mu\text{m}/\text{s}$ in the X direction, and a Y translation step of 100 μm . Under these scanning conditions, the number of laser shots in the X direction is equal to 40 (from equation 1) and due to the accumulation in the Y direction (shift step of 100 μm) the equivalent $N = 320$.

It appears that the surface morphology changes progressively from low roughness mainly due to SiO_x nanoparticles (see reference 24) to organized spikes with typical micron-scale sizes (cases 1 and 2). When the energy is further increased, spikes tend to agglomerate due to SiO_x redeposited materials (case 3). We can conclude that case 1 and case 2 produce the most similar morphology of spikes compared to the previous case (beam accumulation on one spot side).

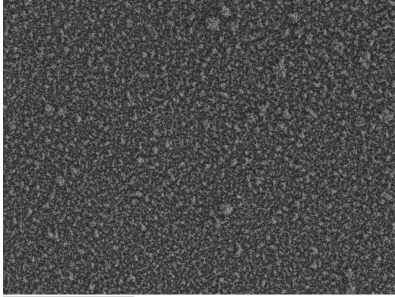
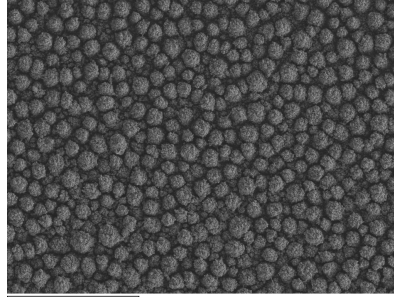
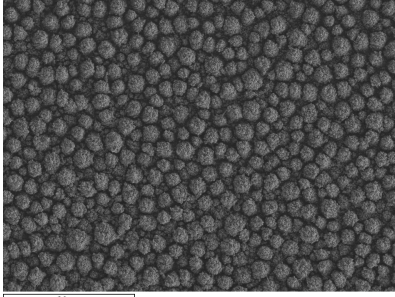
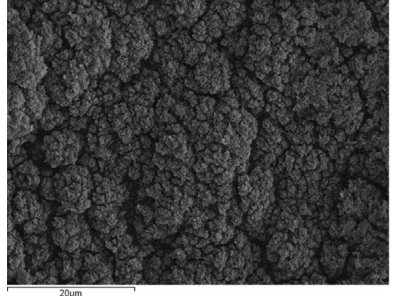
Untreated surface		Case 2 $V_x = 200 \mu\text{m}/\text{s}$ $Y = 100 \mu\text{m}$ E = 2 mJ	
Case 1 $V_x = 200 \mu\text{m}/\text{s}$ $Y = 100 \mu\text{m}$ E = 1 mJ		Case 3 $V_x = 200 \mu\text{m}/\text{s}$ $Y = 100 \mu\text{m}$ E = 5 mJ	

Figure 6: SEM images of large scale untreated and treated MeP-Si surfaces with increasing energy from 1 to 5 mJ (i.e. F from 200 to 1000 mJ/cm^2 , and $N = 320$)

A Bruker Vertex 80v Fourier Transform InfraRed spectrometer (FTIR) [34] in association with the Hyperion 3000 microscope was used to evaluate the reflectivity change with respect to the laser processing parameters. Spectra were acquired from 500 to 8000 cm^{-1} using a standard 15x objective and a Mercury-Cadmium-Telluride detector (MCT) at an instrumental resolution of 4 cm^{-1} . The results are summarized in fig. 7

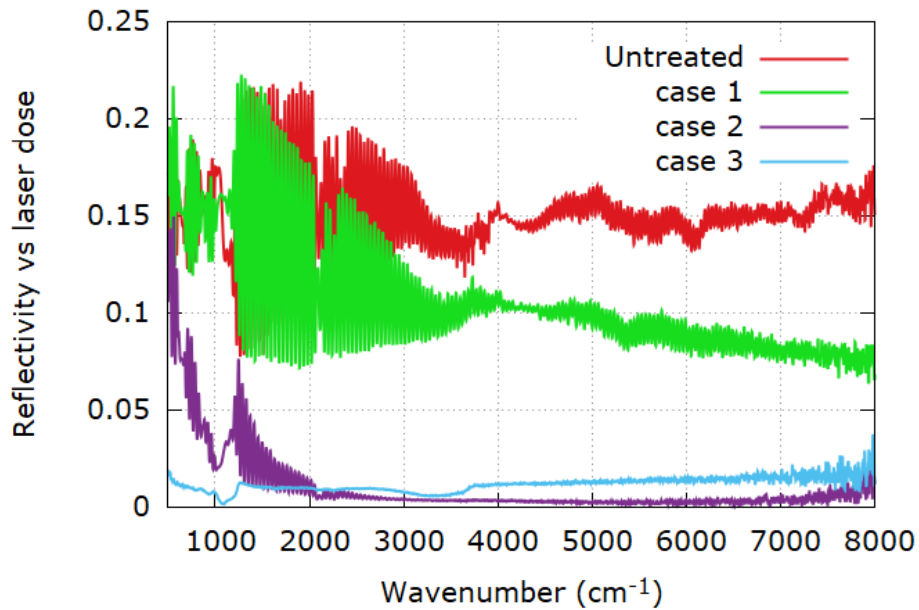


Figure 7: Specular reflectivity spectra of untreated MeP-Si and after laser texturing with laser beam process energy conditions corresponding to cases 1 to 3.

The specular reflectivity spectrum of the untreated sample is typical of an electrochemical-etched layer located at the surface of the silicon wafer [35]. The amplitude and periodicity of the interferences visible in figure 7 are characteristic of a 50 μm thick layer with a porosity around 42%. By increasing the beam energy, the reflectivity spectra decrease in intensity. The increase in the SiOx nanoparticle size present at the sample surface leads to a strengthening of the absorption and light scattering by the sample due to higher roughness. The stronger level of oxidation of the Nps in case 3 is also clearly visible on the corresponding spectrum. The spectral range between 850 and 1300 cm^{-1} and more particularly the strong absorption band located around 1060 cm^{-1} , which is due to the asymmetric Si-O stretching vibration inside a SiO₄ tetrahedron, is evidence of a highly oxidized layer. The decrease in reflectivity between 3000 and 3700 cm^{-1} is the signature of the presence of a high number of hydroxyl groups (case 3). In this particular case ($F = 1000 \text{ mJ/cm}^2$ and $N = 320$), the spikes are destroyed by the high redeposition of SiOx Nps. Finally, Cases 1 and 2 show interesting optical properties (higher absorption with a low oxidation level) for PV or IR-sensing applications.

5. Conclusion

The evolution of the surface morphology of MeP-Si under picosecond laser irradiation at a fixed fluence of 400 mJ/cm^2 was investigated as a function of the number of laser shots. Experimental results showed the enhancement of the shape, distribution and uniformity of spikes when N increases from 10 to 1000. After 1000 shots, *quasi-uniform* conical spikes with an average radius around 1 μm were formed in ambient atmosphere. It was also found that ablation plays the main role in the spike formation. The IR optical characteristics of large-scale MeP-Si spikes were also investigated by FTIR spectroscopy. The results confirm the enhancement of the absorption coefficient in the IR range mainly for cases 1 and 2 that correspond to 200 and 400 mJ/cm^2 and $N = 320$. A higher fluence contributes to a high redeposition rate of SiOx Nps.

Acknowledgement

The authors are very grateful to the French Ministry of Industry and the region 'Centre-Val-de-Loire' for the financial support of this work that is part of the PIA-Tours 2015 National project. The authors would also like to thank Dr. Thierry Sarnet from CNRS for the fruitful discussions on black silicon.

References

- [1] Levchenko I, Ostrikov K. *J. Phys. D. Appl. Phys.* 2007;40(8):2308-2319. doi:10.1088/0022-3727/40/8/S11.
- [2] Garel M, Babonneau D, Boulle A, et al. *Nanoscale* 2015;7(4):1437-1445. doi:10.1039/C4NR05589F.
- [3] Vorobyev AY, Guo C. *Laser Photonics Rev.* 2013;7(3):385-407. doi:10.1002/lpor.201200017.
- [4] Miyazaki K, Miyaji G. *Phys. Procedia* 2012;39:674-682. doi:10.1016/j.phpro.2012.10.088.
- [5] Bonse J, Krüger J, Höhm S, Rosenfeld A. *J. Laser Appl.* 2012;24(4):42006. doi:10.2351/1.4712658.
- [6] Long J, Fan P, Zhong M, Zhang H, Xie Y, Lin C. *Appl. Surf. Sci.* 2014;311:461-467. doi:10.1016/j.apsusc.2014.05.090.
- [7] Varlamova O, Bounhalli M, Reif J. *Appl. Surf. Sci.* 2013;278:62-66. doi:10.1016/j.apsusc.2012.10.140.
- [8] Rebollar E, Vázquez De Aldana JR, Pérez-Hernández JA, Ezquerro TA, Moreno P, Castillejo M. *Appl. Phys. Lett.* 2012;100(4). doi:10.1063/1.3679103.
- [9] Reif J, Martens C, Uhlig S, et al. *Appl. Surf. Sci.* 2015;336:249-254. doi:10.1016/j.apsusc.2014.11.153.
- [10] Shen MY, Crouch CH, Carey JE, Mazur E. *Appl. Phys. Lett.* 2004;85(23):5694-5696. doi:10.1063/1.1828575.
- [11] Huynh TTD, Vayer M, Sauldubois A, Petit A, Semmar N. *Appl. Phys. Lett.* 2015;107(19). doi:10.1063/1.4935413.
- [12] Gräf S, Kunz C, Engel S, Derrien TJ, Müller FA., *Materials (Basel)*. 2018;11(8):1340. doi:10.3390/ma11081340
- [13] Marek Mezera, Martin van Drongelen and G.R.B.E. Römer., *Journal of Laser Micro/Nanoengineering* Vol. 13, No. 2, 2018. doi: 10.2961/jlmm.2018.02.0010.
- [14] A. Talbi, C. Tchiffo Tameko, A. Stolz, E. Millon, C. Boulmer-Leborgne, N. Semmar, *Applied Surface Science*, Volume 418, Part B, 2017, 425-429, doi.org/10.1016/j.apsusc.2017.02.033.
- [15] Crouch CH, Carey JE, Shen M, Mazur E, Génin FY. *Appl. Phys. A Mater. Sci. Process.* 2004;79(7):1635-1641. doi:10.1007/s00339-004-2676-0.
- [16] Halbwax M, Sarnet T, Delaporte P, et al. *Thin Solid Films* 2008;516(20):6791-6795. doi:10.1016/j.tsf.2007.12.117.
- [17] Huang Z, Carey JE, Liu M, Guo X, Mazur E, Campbell JC. *Appl. Phys. Lett.* 2006;89(3):3-5. doi:10.1063/1.2227629.
- [18] Sarnet T, Carey JE, Mazur E. *Int. Symp. High Power Laser Ablation* 2012:219-228. doi:10.1063/1.4739876.
- [19] Branz HM, Yost VE, Ward S, Jones KM, To B, Stradins P. *Appl. Phys. Lett.* 2009;94(23):88-91. doi:10.1063/1.3152244.
- [20] Serpenguzel A, Kurt A, Inanç I, Carey J, Mazur E. *J. Nanophotonics* 2008;2(1):21770. doi:10.1117/1.2896069.
- [21] Crouch CH, Carey JE, Warrender JM, Aziz MJ, Mazur E, Génin FY. *Appl. Phys. Lett.* 2004;84(11):1850-1852. doi:10.1063/1.1667004.
- [22] Baldacchini T, Carey JE, Zhou M, Mazur E. *Langmuir* 2006;22(11):4917-4919. doi:10.1021/la053374k.
- [23] Ma LL, Zhou YC, Jiang N, et al. *Appl. Phys. Lett.* 2006;88(17). doi:10.1063/1.2199593.

- [24] Talbi, A., Kaya-Boussougou, S., Sauldubois, A., Stolz, A., Boulmer-Leborgne, C., Semmar, N., *Applied Physics A: Materials Science and Processing*, 2017, 123 (7), art. no. 463, doi :10.1007/00339-017-1075
- [25] Shen MY, Crouch CH, Carey JE, et al. *Appl. Phys. Lett.* 2003;82(11):1715-1717. doi:10.1063/1.1561162.
- [26] Kam D-H, Kim J, Song L, Mazumder J. *J. Micromechanics Microengineering* 2015;25(4):45007. doi:10.1088/0960-1317/25/4/045007.
- [27] Derrien TJ-Y, Torres R, Sarnet T, Sentis M, Itina TE. *Appl. Surf. Sci.* 2012;258(23):9487-9490. doi:10.1016/j.apsusc.2011.10.084.
- [28] Talbi A, Petit A, Melhem A, et al. *Appl. Surf. Sci.* 2016;374:31-35. doi:10.1016/j.apsusc.2015.09.003.
- [29] Andrei AI, Golosov E V, Yu RK, et al. *Quantum Electron.* 2011;41(9):829. doi 10.1070/Qe2011v041n09abeh014530.
- [30] Langa S, Carstensen J, Christophersen M, et al. *J. Electrochem. Soc.* 2005;152:C525. doi:10.1149/1.1940847.
- [31] Mei H, Wang C, Yao J, et al. Development of novel flexible black silicon. *Opt. Commun.* 2011;284(4):1072-1075. doi:10.1016/j.optcom.2010.10.024.
- [32] Vorobyev AY, Guo C. *Appl. Surf. Sci.* 2011;257(16):7291-7294. doi:10.1016/j.apsusc.2011.03.106.
- [33] Kontermann S, Gimpel T, Baumann AL, Guenther KM, Schade W. *Energy Procedia* 2012;27:390-395. doi:10.1016/j.egypro.2012.07.082.
- [34] De Sousa Meneses D, Eckes M, del Campo L, Santos C. N, Vaills Y, Echegut P, *Vib. Spectrosc.* 2013, 65, 50– 57. doi: 10.1016/j.vibspec.2012.11.01.
- [35] Melhem A, De Sousa Meneses D, Andreazza-Vignolles C, Defforge T, Gautier G, Semmar N, *Structural, J. Phys. Chem. C* 2015, 119, 21443– 21451. doi: 10.1021/acs.jpcc.5b04984.